We are IntechOpen, the world's leading publisher of Open Access books Built by scientists, for scientists

4,800
Open access books available

122,000
International authors and editors

135M
Downloads

Our authors are among the

154
Countries delivered to

TOP 1%
most cited scientists

12.2%
Contributors from top 500 universities

CLARIVATE ANALYTICS BOOK CITATION INDEX INDEXED

WEB OF SCIENCE™

Selection of our books indexed in the Book Citation Index in Web of Science™ Core Collection (BKCI)

Interested in publishing with us?
Contact book.department@intechopen.com

Numbers displayed above are based on latest data collected.
For more information visit www.intechopen.com

9

On-line Cutting Tool Condition Monitoring in Machining Processes using Artificial Intelligence

Antonio J. Vallejo[1], Rubén Morales-Menéndez[2] and J.R. Alique[3]
[1]*Visiting scholar at the Instituto de Automática Industrial, Madrid, Spain*
[2]*Tecnológico de Monterrey, Monterrey NL,*
[3]*Instituto de Automática Industrial, Madrid,*
[1,3]*Spain*
[2]*México*

1. Introduction

High Speed Machining (*HSM*) has become one of the leading methods in the improvement of machining productivity. The term *HSM* covers high spindle speeds, high feed rates, as well as high acceleration and deceleration rates. Furthermore, *HSM* does not imply only working with high speeds but also with high levels of precision and accuracy.

Additional to the *HSM*, many companies producing machine tools are interested in new technologies which provide intelligent features. Several research works (Koren et al., 1999; Erol et al., 2000; Liang et al., 2004) predict that future manufacturing systems will have intelligent functions to enhance their own processes, and the ability to perform an effective, reliable, and superior manufacturing procedures. In the areas of process monitoring and control, these new systems will also have a higher process technology level.

In any typical metal-cutting process, the key indexes which define the product quality are dimensional accuracy and surface roughness; both directly influenced by the cutting tool condition. One of the main goals in a Computer Numerically Controlled (*CNC*) machining centre is to find an *appropriate trade-off* among cutting tool condition, surface quality and productivity. A cutting tool condition monitoring system which optimizes the operating cost with the same quality of the product would be widely appreciated, (Saglam & Unuvar, 2003; Haber & Alique, 2003). For example, in (Tönshoff et al., 1988), it has been demonstrated that effective machining time of the *CNC* milling centre could be increased from 10 to 65% with a monitoring and control system. Also, (Sick, 2002) mentions that any manufacturing process can be significantly optimized using a reliable and flexible tool monitoring system.

The system must develop the following tasks:

- Collisions detection as fast as possible.
- Tool fracture identification.
- Estimation or classification of tool wear caused by abrasion or other influences.

While collision and tool fracture are sudden and mostly unexpected events that require reactions in real-time, the development of wear is a slow procedure. This section focuses on

Source: Robotics, Automation and Control, Book edited by: Pavla Pecherková, Miroslav Flídr and Jindřich Duník,
ISBN 978-953-7619-18-3, pp. 494, October 2008, I-Tech, Vienna, Austria

the estimation of wear. The importance of tool wear monitoring is implied by exchanging worn tools in time, and tool costs can be reduced with a precise exploitation of the tool's lifetime.

However, cutting tool monitoring is not an easy task for several reasons. First, the machining processes are non-linear, and time-variant systems, which makes them difficult to model. Secondly, the acquired signals from sensors are dependent on other kind of factors, such as machining conditions, cutting tool geometry, workpiece material, among others. There is not a direct method for measuring the cutting tool wear, so indirect measurements are needed for its estimation. Besides, signals coming from machine tools sensors are disturbed by many other reasons such as cutting tool outbreaks, chatter, tool geometry variances, workpiece material properties, digitizers noise, sensor nonlinearity, among others. There is not a straightforward solution.

Symbol	Description	Symbol	Description
A	State transition probability distribution	*MFCC*	Mel Frequency Cepstrum Coeff.
AC	Accelerometer	*MR*	Multiple Regression
AE	Acoustic Emission	M	Number of distinct obs. symbols
a_e	Radial depth of cut (mm)	N	Spindle speed (rpm)
a_{ij}	Elements of the transition matrix	N_s	Number of states in the model
ANN	Artificial Neural Networks	N_f	Number of bandpass filters
a_p	Axial depth of cut (mm)	n_p	Number of passes over workpiece
BN	Bayesian Networks	O	Observation sequence of model
B	Obs. symbol probability distribution	q_t	State at time t
CNC	Computer Numerically Controlled	S	State sequence in the model
Curv	Machining geometry curvature(mm^{-1})	*SOFM*	Self-Organizing Feature Maps
DY	Dynamometer	*SP*	Spindle Power
DOE	Design Of Experiments	T	Length of observation sequence
D_{tool}	Diameter of the cutting tool (mm)	T_c	Tool life (min)
FFT	Fast Fourier Transform	T_{mach}	Machining time (min)
FAR	False Alarm Rate	Tr	Training dataset
FFR	False Fault Rate	Ts	Testing dataset
f_{HZ}	Sampling frequency (Hz)	V	Set of individual symbols
f_{Mel}	Scale Mel frequency	VB	Flank wear (mm or μm)
f_z	Feed per tooth (mm/rev/tooth)	VB1	Uniform flank wear (mm o μm)
Fx	Cutting force in x-axis (N)	VB2	Non-uniform wear (mm o μm)
Fy	Cutting force in y-axis (N)	VB3	Localized flank wear (mm o μm)
Fz	Cutting force in z-axis (N)	Vol	Volume of removal metal (mm^3)
HB	Brinell Hardness Number of the workpiece (*BHN*)	x	Sample
HMM	Hidden Markov Models	z	Number of teeth of cutting tool
HSM	High Speed Machining	λ	*HMM* model specification
LVQ	Learning Vector Quantization	π	Initial state distribution for *HMM*
L	Machining length (mm)	μ	Mean value
M	Log bandpass filter output amplitude	σ	Standard deviation

Table 1. Nomenclature.

This work proposes new ideas for the cutting tool condition monitoring and diagnosis with intelligent features (i.e. pattern recognition, learning, knowledge acquisition, and inference from incomplete information). Two techniques will be applied using Artificial Neural

Networks and Hidden Markov Models. The proposal is implemented for peripheral milling process in *HSM.* Table 1 presents all the symbols and variables used in this chapter.

2. State of the art

The cutting tool wear condition is an important factor in all metal cutting processes. However, direct monitoring systems are not easily implemented because their need of ingenious measuring methods. For this reason, indirect measurements are required for the estimation of cutting tool wear. Different machine tools sensors signals are used for monitoring and diagnosing the cutting tool wear condition.

There are important contributions for cutting tool monitoring systems based on Artificial Neural Networks (*ANN)*, Bayesian Network (*BN*), Multiple Regression (*MR*) approaches and stochastic methods.

In (Owsley et al., 1997), the authors presented an approach for monitoring the cutting tool condition. Feature extraction from vibrations during the drilling is generated by Self-Organizing Feature Maps (*SOFM*). The signals processing implies a spectral feature extraction to obtain the time-frequency representation. These features are the inputs of a *HMM* classifier. The authors demonstrated that *SOFM* are an appropriated algorithm for vibration signals feature extraction.

A methodology based on frequency domain is presented by (Chen & Chen, 1999) for on-line detection of cutting tool failure. At low frequencies, the frequency domain presents two important peaks, which are compared to compute a ratio that could be an indicator for monitoring tool breakage.

In (Atlas et al., 2000), the authors used *HMM* for the evaluation of tool wear in milling processes. The feature extraction from vibrations signals were the root mean squared, the energy and its derivative. Two cutting tool conditions were defined: worn and no-worn condition. The reported success was around 93%.

In (Sick, 2002a), a new hybrid technique for cutting tool wear monitoring, which fuses a physical process model with an *ANN* model is proposed for turning. The physical model describes the influence of cutting conditions on measure force signals and it is used to normalize them. The *ANN* model establishes a relationship between the normalized force signals and the wear state of the cutting tool. The performance for the best model was 99.4% for the learning step, and 70.0% for the testing step.

In (Haber & Alique, 2003) is developed an intelligent supervisory system for cutting tool wear prediction using a model-based approach. The dynamic behavior of the cutting force is associated with the cutting tool and process conditions. First, an *ANN* model is trained considering the cutting force, the feed rate, and the radial depth of the cut. Secondly, the residual error obtained from the measure and predicted force is compared with an adaptive threshold in order to estimate the cutting tool condition. This condition is classified as new, half-worn, or worn cutting tool.

In (Saglam & Unuvar, 2003), the authors worked with multilayered *ANN* for the monitoring and diagnosis of the cutting tool condition and surface roughness. The obtained success rates were of 77% for tool wear and 80% for surface roughness.

In (Dey & Stori, 2004), a monitoring and diagnosis approach based on a *BN* is presented. This approach integrates multiple process metrics from sensor sources in sequential machining operations to identify the causes of process variations. It provides a probabilistic

confidence level of the diagnosis. The *BN* was trained with a set of 16 experiments, and the performance was evaluated with 18 new experiments. The *BN* diagnosed the correct state with a 60% confidence level in 16 of 18 cases.
In (Haber et al., 2004) is introduced an investigation of cutting tool wear monitoring in a *HSM* process based on the analysis of different signals signatures in time and frequency domains. The authors used sensorial information from dynamometers, accelerometers, and acoustic emission sensors to obtain the deviation of representative variables. The tests were designed for different cutting speeds and feed rates to determine the effects of a new and worn cutting tool. Data was transformed from time to frequency domain using the Fast Fourier Transform (*FFT*) algorithm. They concluded that second harmonics of tooth path excitation frequency in the vibration signal are the best indicator for cutting tool wear monitoring.
A proposal to exploit speech recognition frameworks in monitoring systems of the cutting tool wear condition is presented in (Vallejo et al., 2005). Also, (Vallejo et al., 2006) presented a new approach for online monitoring the cutting tool wear condition in face milling. The proposal is based on continuous *HMM* classifier, and the feature vectors were computed from the vibration signals between the cutting tool and the workpiece. The feature vectors consisted of the Mel Frequency Cepstrum Coefficients (*MFCC*). The success to recognize the cutting tool condition was 99.86% and 84.55%, for the training and testing dataset, respectively. Also, in (Vallejo et al., 2007) an indirect monitoring approach based on vibration measurements during the face milling process is proposed. The authors compared the performance of three different algorithms: *HMM*, *ANN*, and Learning Vector Quantization (*LVQ*). The *HMM* was the best algorithm with 84.24% accuracy, followed by the *LVQ* algorithm with 60.31% accuracy. Table 2 summarizes all works discussed in this section.

3. Experimental set-up

This research work was focused on covering a domain in mold and die industry with different aluminium alloys. In this industry, the peripheral milling process is of great importance, its geometry can be defined as a simple straight line or even as a different geometry path including concave and convex curvatures.
The experiments took place in a *HSM* centre HS-1000 Kondia, with 25 KW drive motor, three axis, maximum spindle speed 24,000 rpm, and a Siemens open Sinumerik 840D controller, as shown in Figure 1. During the experiment several HSS end mill cutting tools (25° helix angle, and 2-flute) from Sandvik Coromant were selected for the end milling process, and different workpiece materials (Aluminium with hardness from 70 to 157 HBN) were used. These materials were selected because they have important applications in the aeronautic and mold manufacturing industry. Also, several cutting tool diameters (from 8 to 20 mm) were employed.

3.1 Design of experiments

Currently, the most of the research experiments are related to surface roughness and flank wear (VB). In machining processes they only consider a specific combination of cutting tool and workpiece material. Therefore, several authors have pointed out the importance of building databases with information of different materials and cutting tools that allow

computing models by considering a complete domain in the machining process. The *DOE* was defined to consider the most important factors affecting the surface roughness during the peripheral end milling process, see (Vallejo et al., 2007a). Therefore, its results are relevant to compute a surface roughness model as well as and a model to predict the cutting tool condition.

Process	Monitoring States	Sensor Signals	Recognition methods	References
Drilling	Tool wear	AC	HMM	(Owsley et al., 1997)
End Milling	Tool Breakage (Normal, Broke)	AC	FFT	(Chen & Chen, 1999)
End Milling	Tool wear (Worn-no worn)	AC	HMM	(Atlas et al., 2000)
Turning	Tool wear (Wear value)	Process parameters	ANN	Sick, 2002
Turning	Tool wear (New, half worn, worn)	Process parameters	ANN	(Haber & Alique, 2003)
Face Milling	Tool wear (Flank wear)	DY	ANN	(Saglam & Unuvar, 2003)
Face Milling	Tool wear (Low-high)	AE, SP	BN	(Dey & Stori, 2004)
Milling	Tool wear (New, worn)	AE, DY, AC	FFT	(Haber et al., 2004)
Face Milling	Tool wear (New, half-new, half-worn, worn)	AC	HMM	(Vallejo et al., 2006)
Face Milling	Tool wear (New, half-new, half-worn, worn)	AC	HMM, ANN, LVQ	(Vallejo et al., 2007)

Table 2. Comparison of different research efforts for monitoring the cutting tool condition. The recognition method is defined by considering the machining process, sensor signals, and the classification method.

The factors and levels were defined via the application of a screening factorial design over the most important factors affecting the surface roughness. These factors and levels were the following: feed per tooth (f_z), cutting tool diameter (D_{tool}), radial depth of cut (a_e), hardness of the workpiece material (HB), and the machining geometry curvature (Curv). Table 3 shows the factors and levels defined for the experiments. Table 4 presents the selected aluminium alloys with the different cutting tools used in the experiments. The dimensions of the workpiece were 100x170x25 mm, and they were designed to allow the machining of four replicates. The designed geometries are depicted in Figure 2a, and the cutting tools are shown in Figure 2b.

The machining domain in *HSM* was characterized by using different aluminium alloys, cutting tools and several geometries (concave, convex and straight path) in peripheral milling process, and the *DOE* considered the following steps:

1. Run a set of experiments with the cutting tool in sharp condition. During the experimentation the process variables were recorded.
2. Wear the cutting tool with the harder aluminium alloys until reaching a specific flank wear in agreement with ISO-8688 Tool life testing in milling.
3. Run other set of experiments with a different cutting tool wear condition.
4. Repeat the steps 2 and 3 until the cutting tool reaches the tool-life criteria.

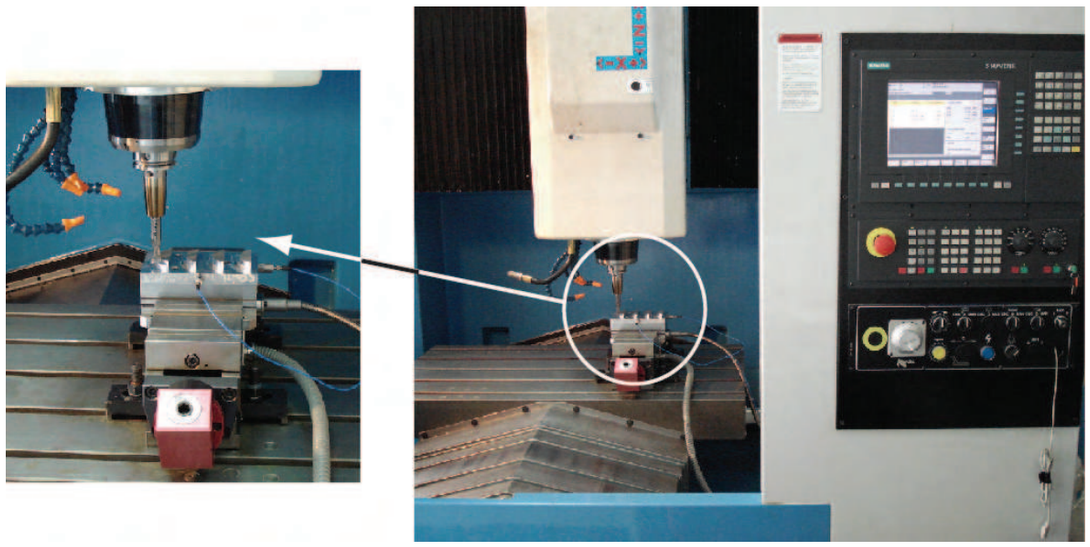

Fig. 1. Experimental Set-up. *CNC* machining centre HS-1000 Kondia (Right side), and the workpiece fixed to the table after the machined process (left side).

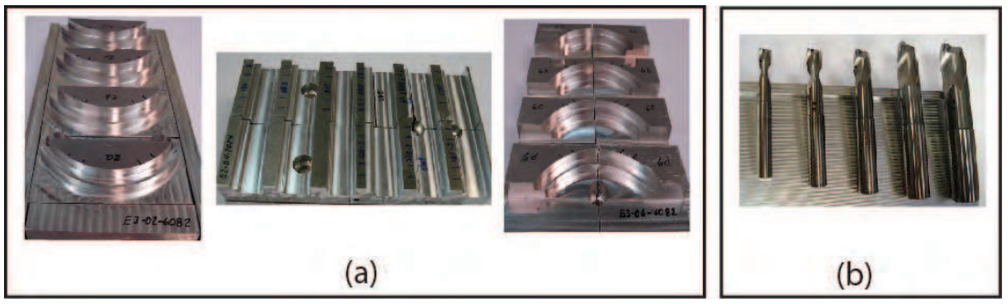

Fig. 2. a) Aluminium workpieces and geometries. b) Cutting tools for the experimentation.

Levels	f_z (mm/rev/tooth)	D_{tool} (mm)	a_e (mm)	HB (BHN)	Curv (mm^{-1})
-2	0.025	8	1	71	-0.05
-1	0.05	10	2	93	-0.025
0	0.075	12	3	110	0
1	0.1	16	4	136	0.025
2	0.13	20	5	157	0.05

Table 3. Factors and levels defined for the experimentation.

Workpiece material Hardness (HB)	Cutting tools Diameter (mm)
5083-H111 (71 HB)	R216.32-08025-AP12AH10F (8 mm)
6082-T6 (93 HB)	R216.32-10025-AP14AH10F (10 mm)
2024-T3 (110 HB)	R216.32-12025-AP16AH10F (12 mm)
7022-T6 (136 HB)	R216.32-16025-AP20AH10F (16 mm)
7075-T6 (157 HB)	R216.32-20025-AP20AH10F (20 mm)

Table 4. Aluminium alloys and specifications of the cutting tools used in the experimentation.

3.2 Tool life evaluation

In practical workshop environment, the time at which a tool ceases to produce workpieces of the desired size or surface quality usually determines the end of useful tool life. It is essential to define tool life as the total cutting time to reach a specified value of tool-life criterion. Here, it is necessary to identify and classify the cutting tool deterioration phenomena, and where it occurs at the cutting edges. The main numerical values of tool deterioration used to determine tool life are the quantity of testing material required and the cost of testing. The following concepts are given to explain the deterioration phenomena in the cutting tool:

- *Tool wear*. Change in shape of the cutting edge part of a tool from its original shape, resulting from progressive loss of tool material during cutting.
- *Brittle fracture (chipping).* Cracks occurrence in the cutting part of a tool followed by the loss of small fragments of tool material.
- *Tool deterioration measure*. Quantity used to express the magnitude of a certain aspect of tool deterioration by a numerical value.
- *Tool-life criterion.* Predetermined value of a specified tool deterioration measure indicating the occurrence of a specified phenomenon.
- *Tool life (T_c).* Total cutting time of the cutting part required to reach a specified tool-life criterion.

In Figure 3, terms related to the tool deterioration phenomena on end milling cutters are shown. These terms include:

- *Flank wear* (VB): Loss of tool material from the tool flanks, resulting in the progressive development of the flank wear land.
- *Uniform flank wear* (VB1): Wear land which is normally of constant width and extends over the tool flanks of the active cutting edge.
- *Non-uniform wear* (VB2): Wear land which has an irregular width and the original flank varies at each position of measurement.
- *Localized flank wear* (VB3): Exaggerated and localized form of flank wear which develops at a specific part of the flank.

The tool-life criterion can be a predetermined numerical value for any type of tool deterioration that can be measured. If there are different forms of deterioration, they should be recorded so when any so when any of the deterioration phenomena limits has been attained, we can say the end of the tool life has been the end of the tool life has been reached.

Predetermined numerical values of specific types of tool wear are recommended:

- For a width of the flank wear land (VB) the following tool life end points are recommended:
  1. Uniform wear: 0.3 mm averaged over all teeth.
  2. Localized wear: 0.5 mm maximum on any individual tooth.
- When chipping occurs, it is to be treated as localized wear using a VB3 value equal to 0.5 mm as a tool-life end point.

Finally, flank wear measurement is carried out parallel to the surface of the wear land and in a perpendicular direction to the original cutting edge. Although the flank wear land on a significant portion of the flank wear may be of uniform size, there will be variations in its value at other portions of the flank, depending on the tool profile and edge chipping. Values of flank wear measurements are related to the area or position along the cutting edges at which the measurement is made.

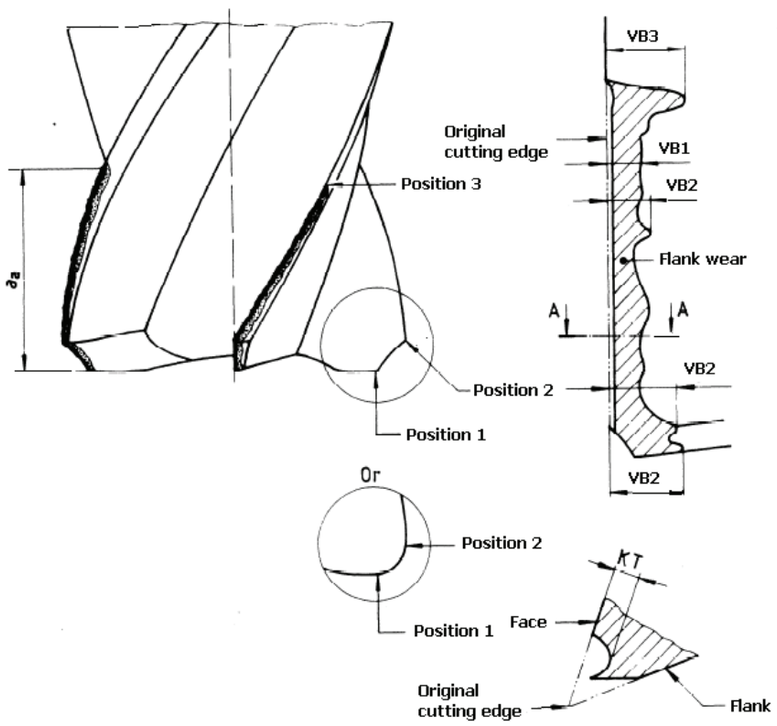

Fig. 3. Different terms in the flank wear are depicted for an end milling cutter (Taken from ISO 8088-2, 1989).

Therefore, it was necessary to define a methodology to wear the cutting tool, and to use the total tool-life during the experimentation. The assessment of the flank wear was taken as tool-life criterion. The applied methodology considers the following steps:

1. The new cutting tools are specified and the *DOE* with the four replicates is made.
2. The flank wear is assessed and registered at the end of the experimentation.
3. The cutting tools are worn by using several workpiece materials, and during the process the flank wear was observed until specific flank wear is reached.
4. The *DOE* is repeated with the new cutting tools conditions.
5. The steps 2, 3 and 4 are repeated (two more times), and the flank wear is measured and registered at the end of the process.

Figure 4 shows the evolution of the tool wear during the experimentation until the maximum tool-life criterion is reached. The experiments were interrupted at regular intervals for measurement of the flank wear (VB). The flank wear pattern along the cutting edge is showed as uniform wear over the surface (see Figure 5). In all cases, the tool wear data corresponds to localized wear.

Milling is an interrupted operation, where the cutting tool edge enters and exits the workpiece several times. The machining time of the tool in minutes was computed by Equation (1):

$$T_{mach} = \frac{L \times n_p}{f_z \times z \times N} \tag{1}$$

The volume of removed material volume was computed by Equation (2):

$$Vol = a_e a_p n_p L \tag{2}$$

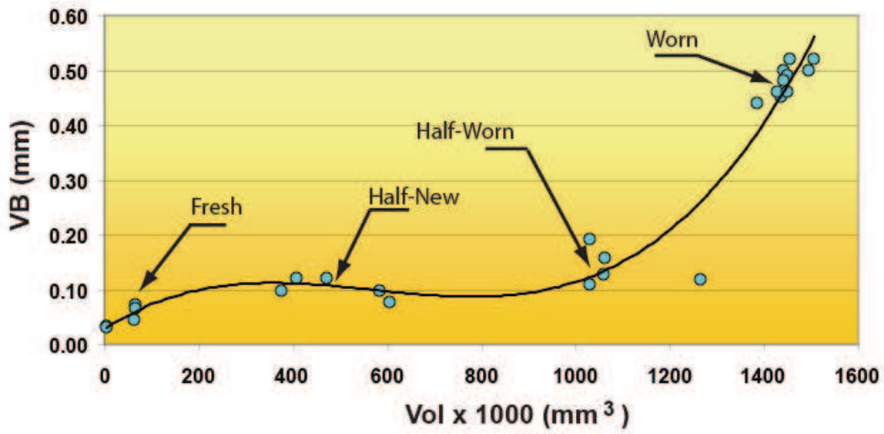

Fig. 4. Evolution of flank wear versus the volume of removal metal. The figure shows the behavior of the five cutting tools.

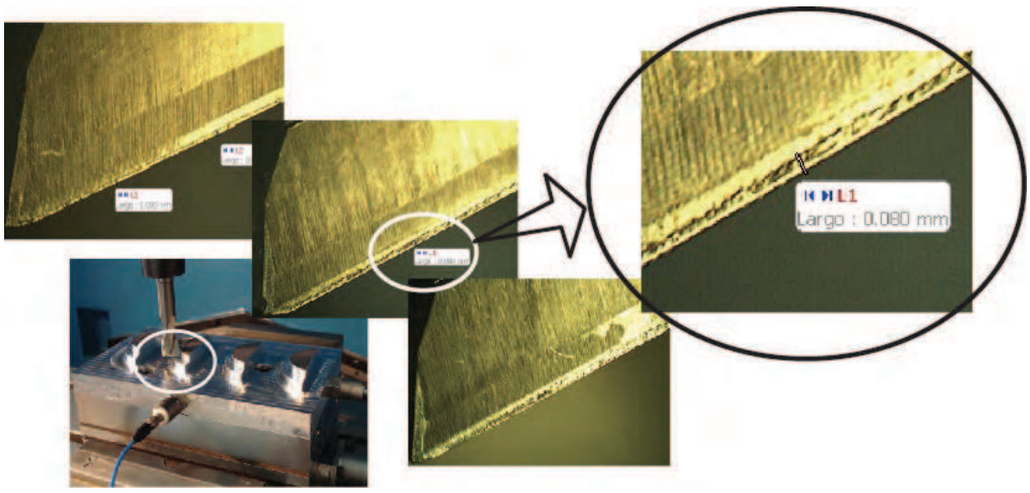

Fig. 5. Evolution of flank wear on the cutting edge. The images were taken throught a stereoscopic microscope. The cutting tool diameter is 12 mm.

The *VB* was selected as the criterion to evaluate the tool's life and its measurement was carried out according to ISO 8688-2, 1989. These two variables, *Vol* and *VB*, define the evolution of the cutting tool wear. The range of the flank wear was selected so that four cutting tool conditions were defined. They are shown in Table 5.

Cutting tool wear condition	Flank wear (mm)
New	$0 \leq VB < 0.08$
Half-new	$0.08 \leq VB < 0.1$
Half-worn	$0.1 \leq VB < 0.3$
Worn	$0.3 \leq VB < 0.5$

Table 5. Cutting tool wear conditions and the flank wear observed during the experimentation.

3.3 Data acquisition system

The Data Acquisition System consists of several sensors that were installed in the *CNC* machine (see Figure 6). For measuring the vibration, 2 PCB Piezotronics accelerometers model 353B04 were fixed in x and y-axis directions on the workpiece. These instruments have a sensitivity of 10 mV/g, in a frequency range from 0.35 to 20,000 Hz. Measurement range is ±500g. Other 2 Bruel and Kjaer piezoelectric accelerometers model 4370, and another model 4371, with a charge sensitivity of 98±2% pC/g, were installed on a ring fixed to the spindle. Also, these sensors allow the recording of vibration in x, y, and z-axis, during the cutting process.

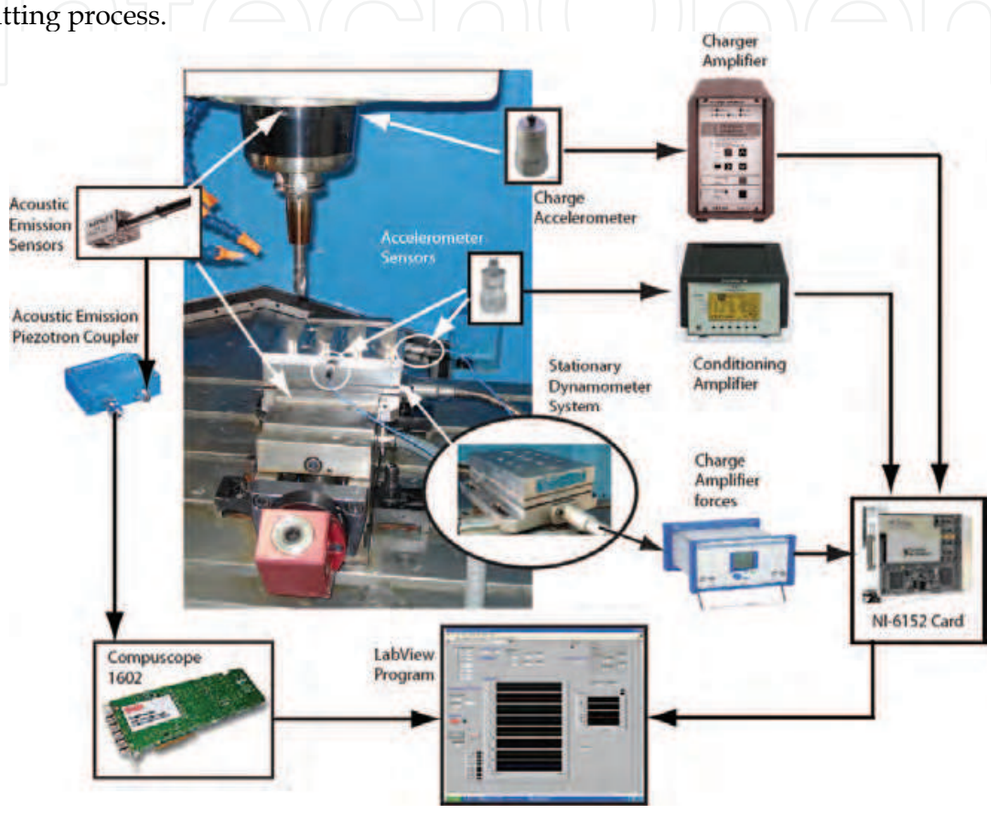

Fig. 6. Experimental Set-up. CNC machining centre and data acquisition system (sensors, amplifiers, boards and LabView interface). The vibration signals of the spindle and workpiece, and forces during machining process were acquired with the NI-6152 board. The acoustic emission signals were acquired with 1602 CompuScope board.

The dynamic cutting force components (Fx, Fy, Fz) were sensed with a 3 component force dynamometer, on which the workpiece was mounted. All the signals were acquired with a high speed multifunction DAQ NI-6152 card, which ensures 16-bit accuracy at a sampling rate of 1.25 MS/s. The system was configured to obtain the signals with a sampling rate of 40,000 samples/s.

The acoustic emissions were recorded with 2 Kistler Piezotron *AE* sensors model 8152B1, with frequency range from 50 to 400 KHz, and sensitivity of 700 V/(m/s). One was installed on a ring fixed to the spindle, and another was installed on the table of the machining centre. The AE signals were acquired with a CompuScope 1602 card for PCI bus, with 16 bit resolution. It provides a dual-channel simultaneous sampling rate of 2.5 MS/s. This board was configured to obtain signals with a sampling rate of 1,000,000 samples/s. The

acquisition system was controlled with a LabView program. This program was used to control the start and end of the recorded signal and storage the information in specific files.

4. Processing of the process variables

Signals from the sensors must be processed to obtain the relevant features which identify the cutting tool condition. Basically, the raw signals undergo three steps in the signal processing:

1. Signal segmentation. During the machining process only one specific segment of the signal was selected and processed. This signal segment was divided into 20 small frames, which correspond to 0.15 (approximately) seconds of the machining time.
2. Features extraction. The feature vectors were computed for all the frames of each signal.
3. Average value. An average value was computed for all frames.

4.1 Feature extraction

The acquired signals during the machining process contain abundant information of the tool status, such as, fundamental frequencies related with the spindle speed and number of inserts, wide band frequency, amplitude of vibration signal, the sensitivity to detect the tool condition, the chatter, and so forth. The different signals are pre-processed calculating their *MFCC* representation, (Deller et al., 1993). This common transformation has shown to be more robust and reliable than other techniques, (Davis & Mermelstaein, 1980). There is a mapping between the real frequency scale (f_{HZ}) and the perceived frequency scale (f_{Mel}). The Mel scale is defined by the following equation

$$f_{Mel} = 2595 \times \log\left(1 + \frac{f_{Hz}}{700}\right) \tag{3}$$

The process to calculate the *MFCC* is shown in Figure 7. In this process, we must define the number of filters (N_f), sampling frequency (f_{HZ}), filters amplitude, and the configuration of the filter banks (triangular or rectangular shape). At the end, the MFCC are computed using the Inverse Discrete Cosine Transform:

$$MFCC_i = \sqrt{\frac{2}{N_f}} \sum_{j=1}^{N} m_j \cos\left(\frac{\pi i}{N_f}(j - 0.5)\right) \tag{4}$$

The result is a seven-dimension vector, where each dimensions correspond to one parameter. *MFCC* were computed by using the VOICEBOX: Speech Processing Toolbox for MatLab, and written by (Brookes, 2006). The routines taken from Speech Recognition module were: (a) The routine *melcepst,* which implements a mel-cepstrum front end for a recognizer; and (b) The routine *melbankm,* which generates the associated bandpass filter matrix.

4.2 MFCC for vibrations and force signals

Specifically for vibrations and force signals, the *MFCC* were computed by considering the following parameters: number of filters 20, sampling rate 40,000 Hz, and a bandpass filter with a triangular shape. The feature vector was of 7 dimensions (1 energy coefficient and 6 MFCC coefficients).

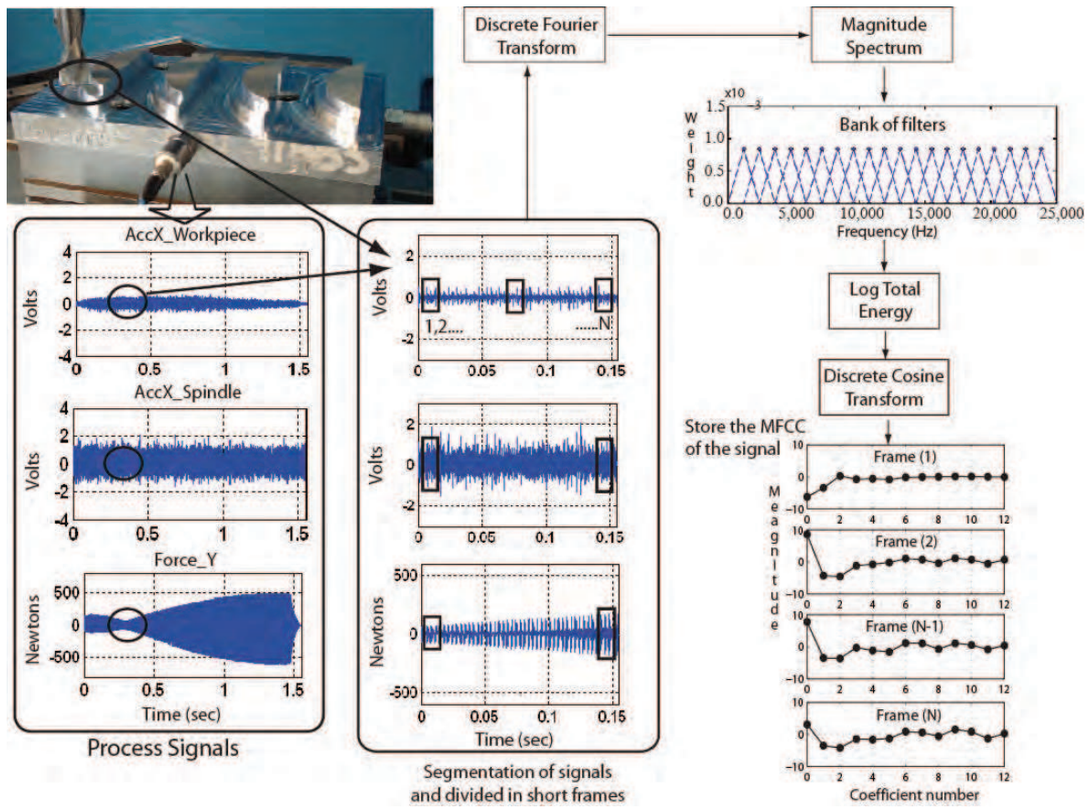

Fig. 7. Feature extraction process. The process variables (signals) are segmented and divided in short frames. A Discrete Fourier Transform and a mapping between the real frequency and the Mel frequency are computed. Then, a bandpass filters bank is applied for smoothing the scaled spectrum. Finally, the *MFCC* are computed using the discrete cosine transform.

4.3 MFCC for acoustic emission signals

MFCC were computed by considering the following parameters: number of filters 20, sampling rate 1,000,000 Hz, and a triangular shape bandpass filter. The feature vector was of 7 dimensions (1 energy coefficient and 6 MFCC coefficients).

5. Monitoring and diagnose the cutting tool wear condition with HMM

Real world processes generally produce observable outputs which can be characterized as signals. The signals can be discrete in nature (e.g., characters from a finite alphabet, quantized vectors from a codebook, etc.), or continuous in nature (e.g., speech samples, temperature measurements, vibration signals, music, etc.). They can be stationary or non-stationary, pure or corrupted from other signal sources. A problem of fundamental interest is characterizing such real-world signals in terms of signal models.

There are many reasons to consider this issue. First, a signal model can provide the basis for the theoretical description of a signal processing system that can be used to process the signal so as to provide a desired output. A second reason why signal models are important is that they are potentially capable of letting us learn a great deal about the signal source. But, the most important reason why signal models are significant is that they often work

extremely well in practice, and enable us to realize important practical systems (e.g. prediction systems, recognition systems, identification systems, among others.).
Signal models can be divided into deterministic and statistical models. Deterministic models generally exploit some known specific properties of the signal, and we only need to determine the values of the signal model parameters (e.g., amplitude, frequency, phase, etc.). On the other hand, statistical models use the statistical properties of the signal. Examples of such statistical models include Gaussian, Poison, Markov, and Hidden Markov processes. In this section, we are going to describe one type of stochastic signal model, namely *HMM*. A complete description of the *HMM* can be found in (Rabiner, 1989; Mohamed & Gader, 2000).

5.1 Discrete Markov Processes

Consider a system which may be described at any time as being in one of a set of N_s distinct states, S_1, S_2, S_3, ..., S_N, as depicted in Figure 8 (where N_s=3). At regularly spaced discrete times, the system undergoes a change of state (possibly back to the same state) according to a set of probabilities associated with the state.
The time instants associated with the state changes are t = 1, 2,...., and the actual state at time t, as q_t. A full probabilistic description of the above system would, in general, require specification of the current state (at time t), as well as all the predecessor states. For the special case of a discrete, first order, Markov chain, this probabilistic description is reduced to just the current and the predecessor state, as shown in the following equation,

$$P[q_t = S_j | q_{t-1} = S_i, q_{t-2} = S_k, \ldots] = P[q_t = S_j | q_{t-1} = S_i] \tag{5}$$

Furthermore we only consider those processes in which the right-hand side of (5) is independent of time, thereby leading to the set of state transition probabilities $a_{i,j}$ of the form

$$a_{ij} = P[q_t = S_j | q_{t-1} = S_i], 1 \le i, j \le N \tag{6}$$

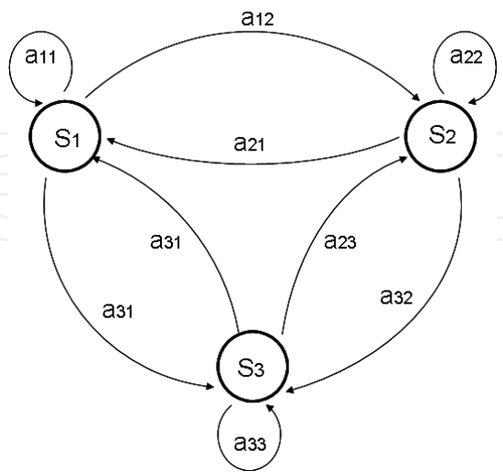

Fig. 8. Representation of a *HMM* with three states and the probabilities of the transition matrix (a_{ij}).

with the state transition coefficients having the properties

$$a_{ij} \geq 0$$

$$\sum_{j=1}^{N} a_{ij} = 1 \tag{7}$$

Because, they obey standard stochastic constraints. The above stochastic process could be called an observation Markov model since the output of the process is the set of states at each instant of time, where each state corresponds to a physical event.

5.2 Extension to Hidden Markov Process

In this part we extend the concept of Markov models to include the case where the observation is a probabilistic function of the state, and the resulting model (which is called a *HMM*) is a doubly embedded stochastic process with an underlying stochastic process that is not observable, but can only be observed through another set of stochastic processes that produce the sequence of observations. To explain this concept, the following example is presented.

Coin Toss Models. Assume that somebody is in a room behind the wall, and he can not see what is happening inside. On the other side of the wall is another person who is performing a coin tossing experiment. The other person will not tell you anything about what he is exactly doing; he will only tell you the result of each coin flip. After a sequence of hidden coin tossing experiments is performed, the observation sequence consisting of a series of heads and tails, would be

$$O=O_1O_2O_3.....O_T \tag{8}$$

$$=H\ H\ J\ J\ J\ H\ J\ J\ H.....H$$

where H stands for heads and J stand for tails. Given the above scenario, the problem of interest is how do we build an *HMM* to explain the observed sequence of heads and tails. The first faced problem is deciding what states in the model correspond with what was observed. Then we should decide how many states should be in the model. One possible choice would be to assume that only a single biased coin was being tossed. In this case we could model the situation with a two-state model where each state corresponds to a side of the coin (i.e., heads or tails). This model is depicted in Figure 9a.

A second form of *HMM* for explaining the observed sequence of coin toss outcomes is given in Figure 9b. In this case there are 2 states in the model and each state corresponds to a different, biased coin being tossed. Each state is defined by a probability distribution of heads and tails. Transitions between states are characterized by a state transition matrix. The physical mechanism which accounts for how state transition is selected could be itself a set of independent coin tosses, or some other probabilistic event.

A third model of *HMM* for explaining the observed sequence of coin toss outcomes is defined very similarly to the *HMM* in Figure 8. This model corresponds to using 3 biased coins, and choosing among them a probabilistic event. Given the opportunity to choose among the three models in Figures 8 and 9 for the explanation of the observed sequence of heads and tails, a natural question would be which model matches the bets the actual observations.

It should be clear that the simple 1-coin model of Figure 9a has only 1 unknown parameter, the model of Figure 9b has four unknown parameters, and the model of Figure 8 has nine

unknown parameters. Thus, with the greater degrees of freedom, the larger *HMMs* would seem to inherently be more capable of modeling a series of coin tossing experiments than it would be equivalent smaller models.

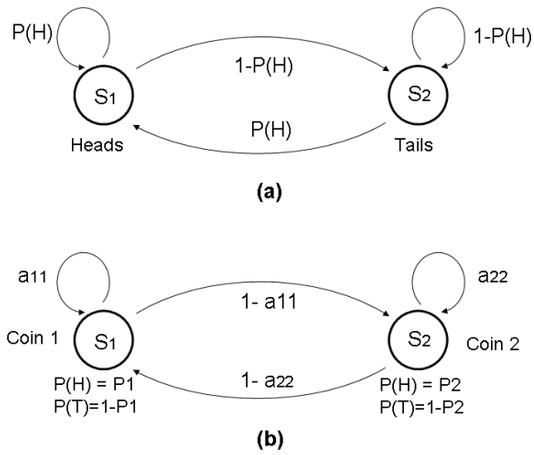

Fig. 9. (a) *HMM* with one coin and the two states. (b) *HMM* with two coins and each state with two observations.

An *HMM* is characterized by the following:

- The number of states in the model, N_s. Generally the states are interconnected in such as way that any state can be reached from any other state. We denote the individual states as $S=S_1,S_2,.....,S_N$, and the state at time t as q_t.
- The number of distinct observation symbols per state, M. The individual symbols such as $V = v_1,v_2,.....,v_M$ (i.e., the symbols in the last example were H (heads) and J (tails)).
- The state transition probability distribution $A = a_{ij}$, where

$$a_{ij} = P[q_t = S_j | q_{t-1} = S_i], 1 \le i, j \le N \tag{9}$$

- The observation symbol probability distribution in state j, $B = b_j(k)$, where

$$b_j(k) = P[v_k \text{ at } t | q_t = S_j],\ 1 \le j \le N,\ 1 \le k \le M \tag{10}$$

The initial state distribution $\pi = \pi_i$ where

$$\pi_i = P[q_1 = S_i], 1 \le i \le N \tag{11}$$

Given appropriate values for N_s, M, A, B, and π, the HMM can be used as a generator of an observation sequence

$$O = O_1O_2,.....,O_T$$

It can be seen from the above discussion that a complete specification of an HMM requires specification of two model parameters (N_s, and M), observation symbols, and three probability measures A, B, and π. For convenience, the compact notation is used,

$$\lambda = (A, B, \pi) \tag{12}$$

to indicate the complete parameter set of the model.

5.3 Baum-Welch algorithm to train the model

The Baum-Welch algorithm, (Rabiner, 1989), is used to adjust the model parameters to maximize the probability of the observation sequence given by the model. The observation sequence used to compute the model parameters is called a training sequence. The training problem is crucial in the applications of the *HMMs*, because it allows us to optimally adapt model parameters to observed training data. The Baum-Welch algorithm is an iterative process that uses the forward and backward probabilities to solve the problem. The goal is to obtain a new model $\bar{\lambda} = (\bar{A}, \bar{B}, \bar{\pi})$ to maximize the function,

$$Q(\lambda, \bar{\lambda}) = \sum_{Q} \frac{P(O, Q|\lambda)}{P(O|\lambda)} \log\left[P(O, Q|\bar{\lambda})\right] \tag{13}$$

First, a current model is defined as $\lambda = (A, B, \pi)$, and used to estimate a new model as $\bar{\lambda} = (\bar{A}, \bar{B}, \bar{\pi})$. The new model must present a better likelihood than the first model to reproduce the observation sequence. Based on this procedure, if we iteratively use $\bar{\lambda}$ in place of λ and repeat the calculus, then we can improve the probability of O being observed from the model until some limiting point is reached.

The result of the recalculation procedure is called a maximum likelihood estimate of the *HMM*. At the end, the new set of parameters (means, variance, and transitions) is obtained for each *HMM*.

5.4 Viterbi algorithm

In pattern recognition applications, it is useful to associate an *optimal* sequence of states to a sequence of observations, given the parameters of the model. In pattern recognition, the feature vector, representing the observations, is known, but the sequence of states that defines the model is unknown. A "reasonable" optimality criterion consists of choosing the state sequence (or path) that brings a maximum likelihood with respect to a given model (i.e., best "explains" the observation). This sequence can be determined recursively via the Viterbi algorithm. This algorithm identifies the single best state sequence, $Q=\{q_1\ q_2\ .....\ q_T\}$ for the given observation sequence $O=\{O_1 O_2\ ....\ O_T\}$, and makes use of two variables:

- The highest likelihood $\delta_t(i)$ along a single path among all the paths ending in state i at time t:

$$\delta_t(i) = \max_{q_1, q_2 \cdots q_{t-1}} P[q_1 q_2 \ldots q_t = i, O_1 O_2 \ldots O_t|\lambda] \tag{14}$$

- A variable $\psi_t(i)$ which allows to keep track of the "best path" ending in state j at time t.

Using these two variables, the algorithm implies the following steps:

1. Initialization

$$\begin{aligned} &\delta_1(i) = \pi_i b_i(O_1) \quad 1 \le i \le N \\ &\psi_i = 0 \end{aligned} \tag{15}$$

2. Recursion

$$\delta_t(j) = \max_{1 \le i \le N_s}[\delta_{t-1}(i) a_{ij}]\, b_j(O_t), \quad 2 \le t \le T,\ 1 \le j \le N_s$$

$$\psi_t(j) = \arg\ \max_{1 \le i \le N_s}[\delta_{t-1}(i) a_{ij}], \quad 2 \le t \le T,\ 1 \le j \le N_s \tag{16}$$

3. Termination:

$$P^* = \max_{1\le i\le N}[\delta_T(i)]$$
$$q_T^* = \arg\max_{1\le i\le N}[\delta_T(i)] \quad (17)$$

4. Path (state sequence) backtracking:

$$q_t^* = \psi_{t+1}(q_{t+1}^*), \quad t = T-1, T-2, \ldots, 1 \quad (18)$$

The Viterbi algorithm delivers the best states path, which corresponds to the observations sequence. This algorithm also computes likelihood along the best path.
The HMM models were computed by using the Hidden Markov Model Toolbox for MatLab. The routines were written by (Murphy, 2005).

6. Results

This section presents the results that were obtained by applying two different artificial intelligence techniques for monitoring and diagnosing the cutting tool condition during the peripheral end milling process in *HSM*: (1) Artificial Neural Network, and (2) Hidden Markov Models. In agreement with the experiments, a database was built with 441 experiments: 110 experiments used a new cutting tool, 112 a half-new cutting tool, 110 a half-worn cutting tool, and 109 a worn cutting tool. A MonteCarlo simulation for the training/testing steps was implemented due to the stochasticity of the approach. The results correspond to the average of 10 runs, where every time a different training data set (*Tr*) and testing data set (*Ts*) was generated (Figure 10).

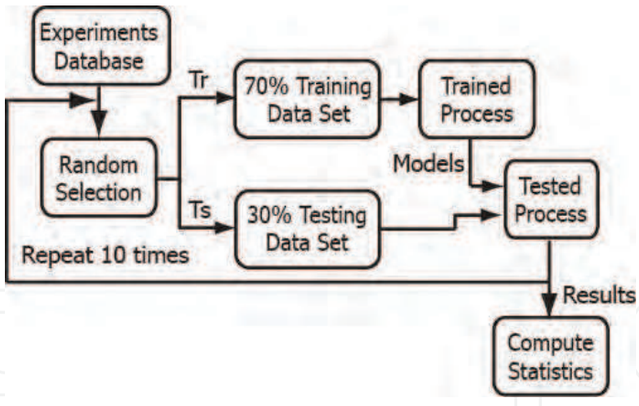

Fig. 10. Procedure for computing the approach performance. A random simulation for splitting the experimental dataset in training/testing sets was implemented due to the stochastic nature of the approaches.

6.1 Artificial neural network

To compare our results with classical approaches, the cutting tool wear condition was modeled with an *ANN* model. The application of *ANN* to on-line process monitoring systems has attracted great interest due to their learning capabilities, noise suppression, and parallel computability. A complete recopilation of research works in on-line and indirect tool wear monitoring with ANN are presented in (Sick, 2002). *ANN* is often defined as a computing

system made up of a number of simple elements called neurons, which possesses information by its dynamic state response to external inputs. The neurons are arranged in a series of layers. Multi-layer feed-forward networks are the most common architecture. Furthermore, there are several learning algorithms for training neural networks. Backpropagation has proven to be successful in many industrial applications and it is easily implemented.
The proposed architecture implies 12 input neurons, one hidden layer with 12 neurons, and 1 output neuron. Figure 11 shows the *ANN* model, where the input neurons represent the following information: feed per tooth, tool diameter, radial depth of cut, workpiece material hardness, curvature, and the *MFCC* vector (7 dimensions).

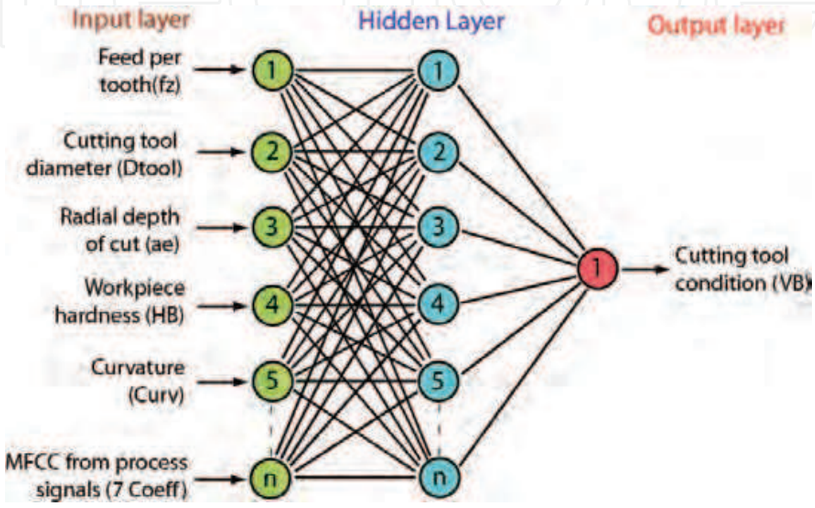

Fig. 11. ANN model implemented for monitoring and diagnosis the on-line cutting tool condition.

We used a feedforward *ANN* model and "tanh" activation function. The trained algorithm was classical backpropagation. For computing, input data (f_z, D_{tool}, a_e, HB, Curv, and *MFCC* vector) was normalized and output data was mapped to [-1, 1]. All the experimental dataset was normalized to avoid numerical inestability. First, the dataset was normalized by considering the mean value (μ), and standard deviation (σ) with the following equation,

$$f(x) = \frac{x - \mu}{\sigma} = \bar{x} \tag{19}$$

A second normalized method was applied: *bipolar sigmoidal*. This method was used because the minimum and maximum values are unknown in real-time. The non-linear transformation prevent most values from being compressed into essentially the same values, and it also compress the large outlier values. The *bipolar sigmoidal* was applied with the following equation:

$$f(\bar{x}) = \frac{1 - e^{(-\bar{x})}}{1 + e^{(-\bar{x})}} \tag{20}$$

With respect to the output neuron, the cutting tool condition, these values were mapped between the normalized tool-wear and tool-wear condition (see Table 6). Finally, the dataset was randomly divided into two sets, training (70%), and testing (30%) sets, in order to measure their generalization capacity.

Normalized tool condition	Cutting tool condition
From +0.66 to +1.00	New
From 0.0 to +0.66	Half-new
From -0.66 to 0.0	Half-worn
From -1.00 to -0.66	Worn

Table 6. Tool-wear from *ANN* model is mapped with the tool-wear Cutting.

The performance of the *ANN* model was computed for ten different sets of data, which were selected in random form. The training and testing processes were programmed by using MatLab software. The obtained results correspond to 8 different ANN models, all of them with the same architecture but different MFCC vector. The MFCC were computed for each of the process signals (accelerometers, forces, and acoustic emission). Table 7 shows the results computed with different process signals. The obtained performance corresponds to an avarage value from the ten data sets.

Data sets	Workpiece		Spindle		X Force	Y Force	AE Spindle	AE Workp.
	Acc-X	Acc-Y	Acc-X	Acc-Y				
Training	90.2%	94.5%	97.8%	98.7%	94.2%	97.6%	99.9%	99.2%
Testing	31.3%	33.8%	40.4%	47.2%	48.5%	48.0%	89.9%	69.7%

Table 7. Performance for the training and testing data sets of the *ANN* model. The first two columns define the success of the accelerometers on the workpiece. The next two, the accelerometers installed on the spindle. The last two columns correspond with the Acoustic Emission sensors.

Table 7 shows that *ANN* model with acoustic emission signal (AE-Spindle) represents the best model for testing dataset, with a performance of 89.9% and Mean Squared Error (*MSE*) of 0.10075. Figure 12 plots the obtained results of the diagnosis system, when the *ANN* model was tested for the prediction of the cutting tool condition.

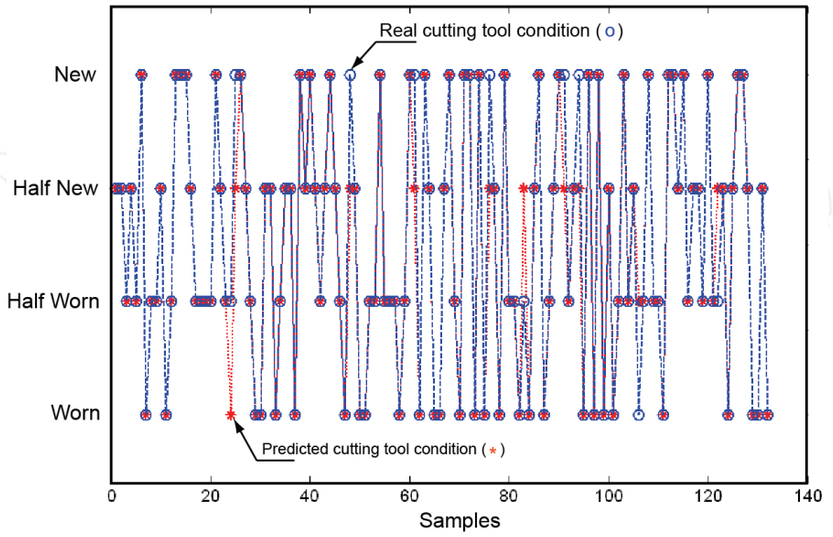

Fig. 12. Diagnosis the cutting tool condition with the ANN(12,12,1) model. The MFCC were computed for the acoustic emission signal (AE-Spindle).

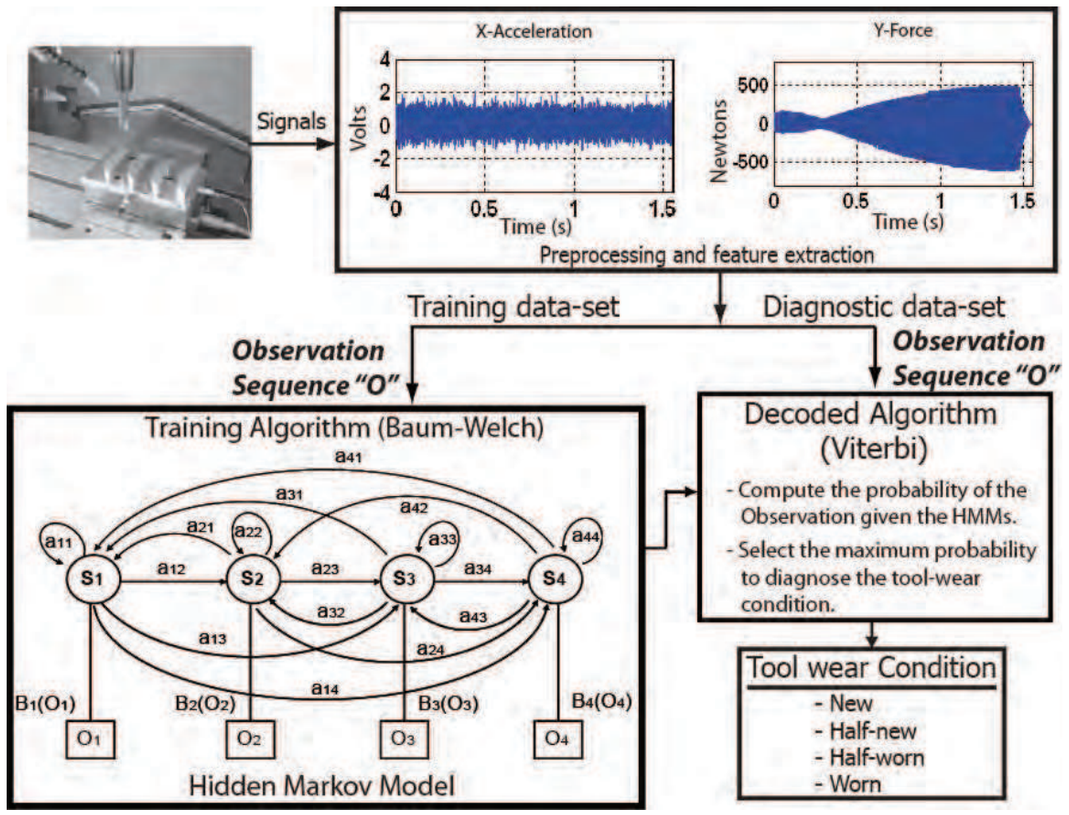

Fig. 13. Flow diagram for monitoring and diagnosis the cutting tool wear condition with continuous HMM. The features from signals are separeted into 2 branches. The training branch leads leads to *HMM*, and the diagnose branch uses the new observations and *HMM*s to recognize the cutting tool condition.

6.2 Hidden Markov Model

Figure 13 shows the flow diagram implemented for monitoring and diagnosing the cutting tool wear condition on-line with the *HMM* model. First, the signals are processed and splited into two: training and testing branches. Second, the training branch produces the *HMM* parameters by using the Baum-Welch algorithm. In this case, four models were computed to represent the four cutting tool conditions. Third, the testing branch uses the preprocessed signals and the HMM to compute the $P(O/\lambda)$ using the Viterbi algorithm for each model. The model with higher probability is selected as result.

The *HMM* framework was evaluated for different states and Gaussians in order to find the optimum performance results. Three different configurations were defined with seven MFCC:

1. *HMM* with 3 states and 2 Gaussians
2. *HMM* with 4 states and 2 Gaussians
3. *HMM* with 4 States and 4 Gaussians.

Figure 14 shows how the performance increases by increasing the states and Gaussians in the *HMM* approach. Based on this result, the selected configuration was with 4 states and 2 Gaussians, where the average performance was 77.51% for testing dataset. The process signal was the *AE* installed over the table.

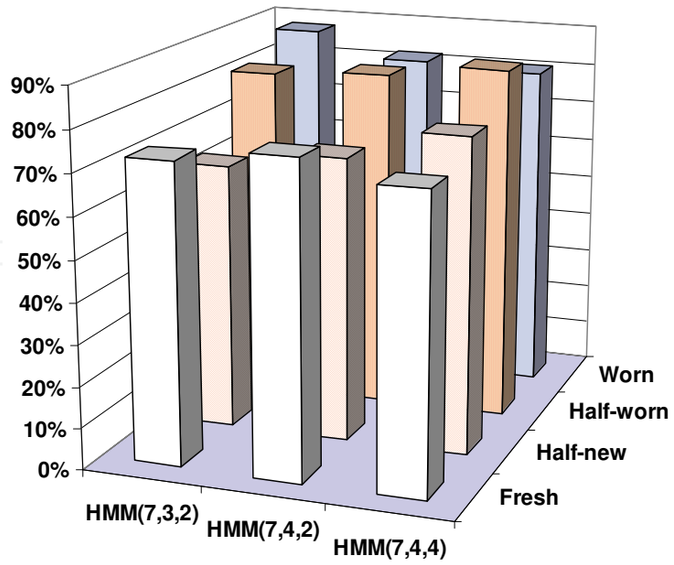

Fig. 14. Perfomance of the HMM with different configuration. The *HMM* were computed with different number of states (3, 4) and Gaussians (2,4).

Figure 15 shows the performance of the *HMMs* with the different signals. The acoustic emission signals present the best performance. For the AE-Spindle signal, the average performance was 99.4% for training dataset, and 95.1% for testing dataset.

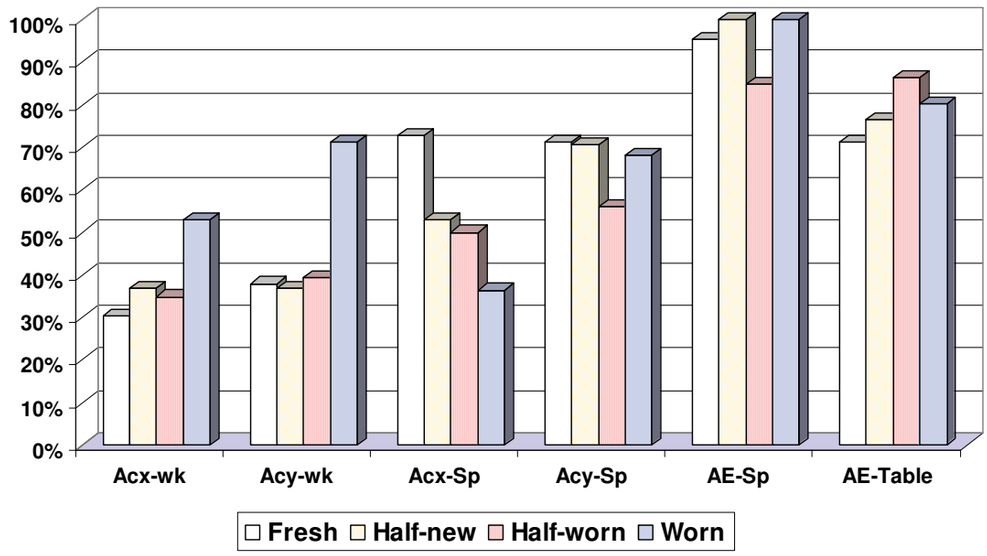

Fig. 15. Performance of the *HMM* for the different process signals. The results correspond to the obtained success for the testing dataset.

A classical test in a diagnosis system is to identify two alarms due to a false classification of cutting tool condition. These alarms are: False Alarm Rate (*FAR*), and False Fault Rate (*FFR*).

FAR condition represents a damage tool, but it is not true. *FFR* condition corresponds to a good state of the tool, but it is really damaged. The *FAR* condition is not a problem for diagnosis, but it reduces the productivity. However, the *FFR* condition might represent an expensive problem when the rate is high, because the tool can break before it is replaced. Figure 16 shows the misclassification percentage due to the *FFR* condition. The classifier with the lower percentage of the *FFR* was the *HMM* using the acoustic emission sensor. Once again, the AE-spindle does not produce any *FFR* condition.

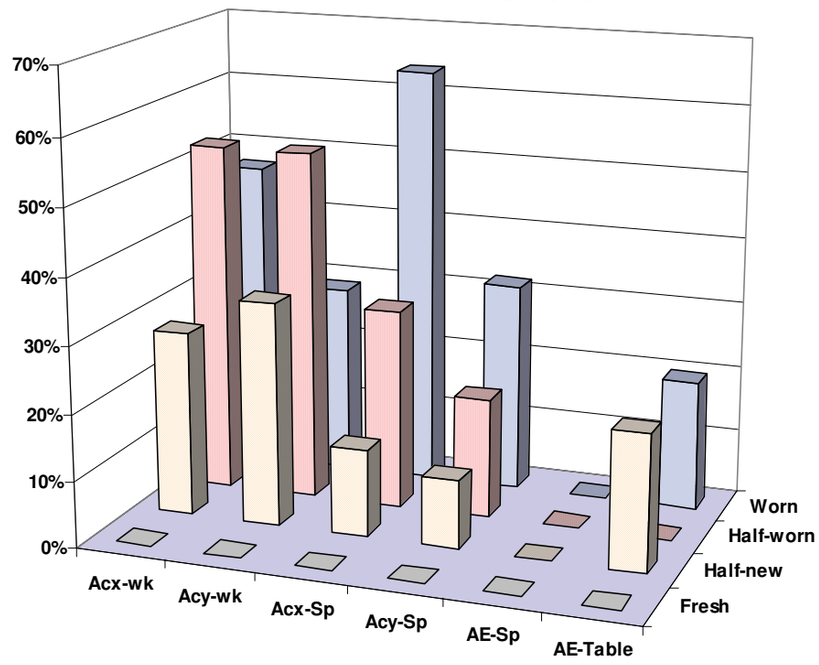

Fig. 16. Misclassification percentage in FFR alarms, for the *HMM* with different process signals.

7. Conclusions

This chapter presented new ideas for monitoring and diagnosis of the cutting tool condition with two different algorithms for pattern recognition: *HMM*, and *ANN*. The monitoring and diagnosis system was implemented for peripheral milling process in *HSM,* where several Aluminium alloys and cutting tools were used. The flank wear (VB) was selected as the criterion to evaluate the tool's life and four cutting tool conditions were defined to be recognized: New, half new, half worn, and worn condition.

Several sensors were used to record important process variables; accelerometer, dynamometer, and acoustic emission. Feature vectors, based on the Mel Frequency Cepstrum Coefficients, were computed to characterize the process signals during the machining processes. First, with the cutting parameters and *MFCC*, the cutting tool condition was modeled with an *ANN* model. The feedfoward *ANN* model and backpropagation algorithm were used to define the *ANN* model. The proposed architecture implies 12 input neurons and one output neuron (cutting condition). The best results were obtained by using the signals from the Acoustic Emission installed on the machine spindle. The success rate for the *ANN* model was 89.9% for the testing dataset.

Second, the *HMM* approach was configured with four states and two Gaussians, and the *HMM* models were computed with each one of the process signals. The best result was obtained with the signals coming from *AE*-Spindle. The performance was 95.08% for testing dataset, and 0.0% in the *FFR* condition. It is very important to mention, that *HMM* approach only uses one sensor to classify the cutting tool condition, while the ANN approach uses sensor fusion of five cutting parameters and one process variable to get the reported performance.

8. References

Atlas, L., Ostendorf, M., and Bernard, G. D., (2000). Hidden Markov Models for Machining Tool-Wear. *IEEE*, pp. 3887-3890.

Brookes, M., (2006). VOICEBOX: Speech Processing Toolbox for MatLab (http://www.ee.ic.ac.uk/hp/staff/dmb/voicebox/voicebox.html), Exhibition Road, London SW7 2BT, UK.

Chen, J.C., and Chen, W. (1999). A Tool Breakage Detection System using an Accelerometer Sensor. *J. of Intelligent Manufacturing*, 10(2), pp. 187-197.

Davis, B.S., and Mermelstaein P., (1980). Comparison of Parametric Representation for Monosyllabic Word Recognition in Continuously Spoken Sentences. *IEEE Transactions on Acoustic, Speech, and Signal Processing*, 4(28), pp. 357-366.

Deller, J.R., Hansen, J.H., and Proakis, J.G., (1993). Discrete-Time Processing of Speech Signals. *IEEE pres*, NJ 08855-1331.

Dey, S., and Stori, J.A. (2004). A Bayesian Network Approach to Root Cause Diagnosis of Process Variations. *International Journal of Machine Tools & Manufacture*, (45), pp. 75-91.

Erol, N.A., Altintas, Y., and Ito, M.R. (2000). Open System Architecture Modular Tool Kit for Motion and Machining Process Control. *IEEE/ASME Transactions on Mechatronics*, 5(3), pp. 281-291.

Haber, R.E. and Alique, A. (2003). Intelligent Process Supervision for Predicting Tool Wear in Machining Processes. *Mechatronics*, (13), pp. 825-849.

Haber, R.E., Jiménez, J.E., Peres, C.R., and Alique, J.R. (2004). An Investigation of Tool-Wear Monitoring in a High-Speed Machining Process. *Sensors and Actuators A*, (116), pp. 539-545.

ISO 8688-2, (1989). Tool Life Testing in Milling – Part 2: End Milling. *International Standard*, first edition.

Korem, Y., Heisel, U., Jovane, F., Moriwaki, T., Pritschow, G., Ulsoy, G. and Van Brussel, H. (1999). Reconfigurable Manufacturing Systems. *Annals of the CIRP* 48(2) , pp. 527-540.

Liang, S.Y., Hecker, R.L., and Landers, R.G. (2004). Machining Process Monitoring and Control: the State of the Art. *Manufacturing Science and Engineering*, 126, pp. 297-310.

Mohamed, M.A., and Gader, P., (2000). Generalized Hidden Markov Models - Part I: Theoretical Frameworks. IEEE Transactions on Fuzzy Systems, 8(1), pp. 67-81.

Murphy, K., (2005). Hidden Markov Model Toolbox for MatLab (http://www.cs.ubc.ca/~murphyk/Software/HMM/hmm.html).

Owsley, L.M., Atlas, L.E., and Bernard, G.D. (1997). Self-Organizing Feature Maps and Hidden Markov Models for Machine-Tool Monitoring. *IEEE Transactions on Signals Processing*, 45(11), pp. 2787-2798.

Rabiner, L.R., (1989). A Tutorial on Hidden Markov Models and Selected Applications in Speech Recognition. *Proceedings of the IEEE*. 77(2), pp. 257-286.

Saglam, H., and Unuvar, A. (2003). Tool Condition Monitoring in Milling based on Cutting Forces by a Neural Network. *International Journal of Production Research*, 41(7), pp. 1519-1532.

Sick, B. (2002). On-Line and Indirect Tool Wear Monitoring in Turning with Artificial Neural Networks: A review of more than a decade of research. *Mechanical Systems and Signal Processing*, 16(4), pp. 487-546.

Sick, B. (2002a). Fusion of Hard and Soft Computing Techniques in Indirect, Online Tool Wear Monitoring. *IEEE Transactions of Systems, Man, and Cybernetics*, 32(2), pp. 80-91.

Tönshoff, H.K., Wulfsberg, J.P., Kals, H.J., König, W., and Van Luttervelt, C.A. (1988). Developments and Trends in Monitoring and Control of Machining Processes. *Annals of the CIRP*, 37(2), pp. 611-622.

Vallejo, A.J., Nolazco-Flores, J.A., Morales-Menéndez, R., Sucar, L.E., and Rodríguez, C.A., (2005). Tool-wear Monitoring based on Continuous Hidden Markov Models. *LNCS 3773 Springer-Verlag, X CIARP.,* pp. 880-890.

Vallejo, A.J., Morales-Menéndez, R., Rodríguez, C.A., and Sucar, L.E., (2006). Diagnosis of a Cutting Tool in a Machining Center. *IEEE International Joint Conference on Neural Networks*, pp. 7097-7101.

Vallejo, A.J., Morales-Menéndez, R., Garza-Castañon, L.E., and Alique, J.R., (2007). Pattern Recognition Approaches for Diagnosis of Cutting Tool Wear Condition. *Transactions of the North American Manufacturing of Research Institution of SME,* 35, pp. 81-88.

Vallejo, A.J., Morales-Menéndez, and Alique, J.R., (2007a). Designing a Cost-effective Supervisory Control System for Machining Processes. *IFAC-Cost effective Automation in Networked Product Development and Manufacturing*, IFAC-PapersOnLine.

Vallejo, A.J., Morales-Menéndez, R., and Alique, J.R., (2008). Intelligent Monitoring and Decision Control System for Peripheral Milling Process. *To appear in IEEE International Conference on Systems, Man, and Cybernetics,* October, 2008.

Robotics Automation and Control

Edited by Pavla Pecherkova, Miroslav Flidr and Jindrich Dunik

ISBN 978-953-7619-18-3
Hard cover, 494 pages
Publisher InTech
Published online 01, October, 2008
Published in print edition October, 2008

This book was conceived as a gathering place of new ideas from academia, industry, research and practice in the fields of robotics, automation and control. The aim of the book was to point out interactions among various fields of interests in spite of diversity and narrow specializations which prevail in the current research. The common denominator of all included chapters appears to be a synergy of various specializations. This synergy yields deeper understanding of the treated problems. Each new approach applied to a particular problem can enrich and inspire improvements of already established approaches to the problem.

How to reference

In order to correctly reference this scholarly work, feel free to copy and paste the following:

Antonio J. Vallejo, Rubén Morales-Menéndez and J.R. Alique (2008). On-line Cutting Tool Condition Monitoring in Machining Processes Using Artificial Intelligence, Robotics Automation and Control, Pavla Pecherkova, Miroslav Flidr and Jindrich Dunik (Ed.), ISBN: 978-953-7619-18-3, InTech, Available from: http://www.intechopen.com/books/robotics_automation_and_control/on-line_cutting_tool_condition_monitoring_in_machining_processes_using_artificial_intelligence

INTECH
open science | open minds

InTech Europe
University Campus STeP Ri
Slavka Krautzeka 83/A
51000 Rijeka, Croatia
Phone: +385 (51) 770 447
Fax: +385 (51) 686 166
www.intechopen.com

InTech China
Unit 405, Office Block, Hotel Equatorial Shanghai
No.65, Yan An Road (West), Shanghai, 200040, China
中国上海市延安西路65号上海国际贵都大饭店办公楼405单元
Phone: +86-21-62489820
Fax: +86-21-62489821

IntechOpen